Fine particulate matter (PM$_{2.5}$) trends in China, 2013-2018: separating contributions from anthropogenic emissions and meteorology

Shixian Zhai[1,2], Daniel J. Jacob[2], Xuan Wang[2], Lu Shen[2], Ke Li[2], Yuzhong Zhang[2], Ke Gui[3], Tianliang Zhao[1], Hong Liao[4]

[1]Key Laboratory for Aerosol-Cloud-Precipitation of China Meteorological Administration, Collaborative Innovation Center on Forecast and Evaluation of Meteorological Disasters, School of Atmospheric Physics, Nanjing University of Information Science & Technology, Nanjing 210044, China

[2]John A. Paulson School of Engineering and Applied Sciences, Harvard University, Cambridge, Massachusetts 02138, USA

[3]Key Laboratory for Atmospheric Chemistry, Chinese Academy of Meteorological Sciences, CMA, Beijing 100081, China

[4]Jiangsu Key Laboratory of Atmospheric Environment Monitoring and Pollution Control, Collaborative Innovation Center of Atmospheric Environment and Equipment Technology, School of Environmental Science and Engineering, Nanjing University of Information Science & Technology, Nanjing 210044, China

Correspondence to: Shixian Zhai (zhaisx@g.harvard.edu).

Abstract. Fine particulate matter (PM$_{2.5}$) is a severe air pollution problem in China. Observations of PM$_{2.5}$ have been available since 2013 from a large network operated by the China National Environmental Monitoring Center (CNEMC). The data show a general 30-50% decrease of annual mean PM$_{2.5}$ across China over the 2013-2018 period, averaging -5.2 µg m^{-3} a^{-1}. Trends in the five megacity cluster regions targeted by the government for air quality control are -9.3 ± 1.8 µg m^{-3} a^{-1} (± 95% confidence interval) for Beijing-Tianjin-Hebei, -6.1 ± 1.1 µg m^{-3} a^{-1} for Yangtze River Delta, -2.7 ± 0.8 µg m^{-3} a^{-1} for Pearl River Delta, -6.7 ± 1.3 µg m^{-3} a^{-1} for Sichuan Basin, and -6.5 ± 2.5 µg m^{-3} a^{-1} for Fenwei Plain (Xi'an). Concurrent 2013-2018 observations of sulfur dioxide (SO$_2$) and carbon monoxide (CO) show that the declines in PM$_{2.5}$ are qualitatively consistent with drastic controls of emissions from coal combustion. However, there is also a large meteorologically driven interannual variability of PM$_{2.5}$ that complicates trend attribution. We used a stepwise multiple linear regression (MLR) model to quantify this meteorological contribution to the PM$_{2.5}$ trends across China. The MLR model correlates the 10-day PM$_{2.5}$ anomalies to wind speed, precipitation, relative humidity, temperature, and 850 hPa meridional wind velocity (V850). The meteorology-corrected PM$_{2.5}$ trends after removal of the MLR meteorological contribution can be viewed as driven by trends in anthropogenic emissions. The mean PM$_{2.5}$ decrease across China is -4.6 µg m^{-3} a^{-1} in the meteorology-corrected data, 12% weaker than in the original data, meaning that 12% of the PM$_{2.5}$ decrease in the original data is attributable to

meteorology. The trends in the meteorology-corrected data for the five megacity clusters are -8.0 ± 1.1 µg m^{-3} a^{-1} for Beijing-Tianjin-Hebei (14% weaker than in the original data), -6.3 ± 0.9 µg m^{-3} a^{-1} for Yangtze River Delta (3% stronger), -2.2 ± 0.5 µg m^{-3} a^{-1} for Pearl River Delta (19% weaker), -4.9 ± 0.9 µg m^{-3} a^{-1} for Sichuan Basin (27% weaker), and -5.0 ± 1.9 µg m^{-3} a^{-1} for Fenwei Plain (Xi'an; 23% weaker). 2015-2017 observations of flattening PM$_{2.5}$ in the Pearl River Delta and increases in the Fenwei Plain can be attributed to meteorology rather than to relaxation of emission controls.

1. Introduction

PM$_{2.5}$ (particulate matter with aerodynamic diameter less than 2.5µm) is a severe air pollution problem in China, responsible for 1.1 million excess deaths in 2015 (Cohen et al., 2017). The Chinese government introduced in 2013 the Action Plan on the Prevention and Control of Air Pollution (Chinese State Council, 2013a), called Clean Air Action for short, to aggressively control anthropogenic emissions. Starting that year, PM$_{2.5}$ data from a nationwide monitoring network of about 1,000 sites became available from the China National Environmental Monitoring Center (CNEMC) of the Ministry of Ecology and Environment of China (MEEC). These data show 30-40% decreases of PM$_{2.5}$ across eastern China over the 2013-2017 period (Chinese State Council, 2018a; X. Zhang et al., 2019). However, interpretation of these trends in terms of emission controls may be biased by interannual variability and trends in meteorology (R. Zhang et al., 2014; Y. Wang et al., 2014; Zhu et al., 2012; Jia et al., 2015; Li et al., 2018; Yang et al., 2018; Yang et al., 2016; Liang et al., 2016; Cheng et al., 2019; Chen et al., 2019; Silver et al., 2018). Here we use a stepwise multi-linear regression (MLR) model to separate the effects of meteorological variability and emission controls on the 2013-2018 trends in PM$_{2.5}$ across China.

Meteorology drives large day-to-day, seasonal, and interannual variations in PM$_{2.5}$ in China by affecting transport, scavenging, emissions, and chemical production (Y. Wang et al., 2014; Leung et al., 2018; Tai et al., 2012; Zou et al., 2017). The relationships between PM$_{2.5}$ and meteorological variables are complex and differ by region and time of year (Shen et al., 2017). For example, wintertime PM$_{2.5}$ pollution events in central and eastern China are associated with low wind speed and high relative humidity (RH) (Y. Wang et al., 2014; R. Zhang et al., 2014; Pendergrass et al., 2019; Moch et al., 2018; Song et al., 2019). On the other hand, high wind speeds in northern China in spring and summer promote dust emission (Lyu et al., 2017; X. Wang et al., 2004). Precipitation scavenging is a major factor driving PM$_{2.5}$ variability in southern and coastal China (Chen et al., 2018; Leung et al., 2018).

Anthropogenic emissions of PM$_{2.5}$ and its precursors including sulfur dioxide (SO$_2$), nitrogen oxides (NO$_x$), ammonia (NH$_3$), and nonmethane volatile organic compounds (NMVOCs) have undergone large changes in China over the past decades. Rapid growth in emissions from 1980 to 2006 led to a general increase in PM$_{2.5}$ over China, as demonstrated by visibility

data (Che et al., 2007; Han et al., 2016; Wang and Chen, 2016; Fu et al., 2014; X. Zhang et al., 2012) and since 1999 by satellite aerosol optical depth (AOD) data (Ma et al., 2016; Lin et al., 2018; Zhao et al., 2017). SO_2 emissions peaked in 2006/2007, NO_x emissions peaked in 2011, and NH_3 emissions peaked around 1996, as estimated from emission inventories (Zhao et al., 2017; J. Wang et al., 2017; Xia et al., 2016; F. Liu et al., 2016a; Lu et al., 2010; Xu et al., 2016; Kang et al., 2016) and observed from satellites (Xia et al., 2016; F. Liu et al., 2016a; de Foy et al., 2016; van der A et al., 2017). SO_2 and NO_x emissions have declined since their peaks, whereas NH_3 emissions have remained relatively stable since its peak (Zhao et al., 2017). The onset of emission controls led to slight decreases in $PM_{2.5}$ over the 2006-2012 period as indicated by satellite AOD data (Ma et al., 2016; Lin et al., 2018; Zhao et al., 2017; Ma et al., 2019) and surface observations (Tao et al., 2017; J. Wang et al., 2017). The Clean Air Action greatly increased the scope of emission controls. The Multi-resolution Emission Inventory for China (MEIC, http://www.meicmodel.org) estimates nationwide emission decreases over the 2013-2017 period of 59% for SO_2, 33% for primary $PM_{2.5}$, 21% for NO_x, and 3% for NH_3, with NMVOCs increasing by 2% (Zheng et al., 2018). Continued reductions in emissions are required and implemented in 2018 (Chinese State Council, 2018b). Our goal in this work is to quantify the response of $PM_{2.5}$ to these rapid emission changes by resolving the effect of meteorological variability, thus allowing improved assessment of the success of the Clean Air Action.

2. Data and methods

2.1. Observations

We use 2013-2018 hourly data for surface air $PM_{2.5}$ together with SO_2, nitrogen dioxide (NO_2), and CO concentrations from the CNEMC network (http://106.37.208.233:20035/). The network started in January 2013 with 496 sites in 74 major cities across the country (Chinese State Council, 2013b), growing to ~1500 sites in 454 cities by 2018. $PM_{2.5}$ mass concentrations are measured using the micro oscillating balance method and/or the β absorption method (MEP, 2012; Zhang and Cao, 2015). SO_2, NO_2, and CO concentrations are measured at the same sites as $PM_{2.5}$. NO_2 concentrations are measured by the molybdenum converter method known to have positive interferences from NO_2 oxidation products (Dunlea et al., 2007). SO_2 and CO are respectively measured using ultraviolet fluorescence and infrared absorption (MEP, 2012; Zhang and Cao, 2015). We applied quality control to the hourly CNEMC data following Barrero et al. (2015) to exclude severe outliers. There are also occasional consecutive repeats of data that may be caused by faulty instruments or reporting (Rohde and Muller, 2015; Silver et al., 2018). Here we removed values from the hourly time series when there are >24 consecutive repeats. These in whole removed 7.4%, 7.0%, 6.4%, and 6.7% of the $PM_{2.5}$, SO_2, NO_2, and CO data respectively.

We correlated these air quality observations with meteorological observations from 839 stations distributed across China (Figure S1) and compiled in the Surface Daily Climate Dataset (V3.0) released by the China National Meteorological Information Center (CNMIC; http://data.cma.cn/). These include data for wind speed (WDS), precipitation (PRECIP), relative humidity (RH), and temperature (TEM). We also used the 850-hPa meridional wind velocity (V850) from the MERRA-2 reanalysis produced at 0.5°x0.625° horizontal resolution by the NASA Global Modeling and Assimilation Office (https://gmao.gsfc.nasa.gov/reanalysis/MERRA-2). We choose these meteorological variables for their strong correlations with $PM_{2.5}$ identified in previous studies (Y. Wang et al., 2014; Cai et al., 2017; Shen et al., 2017; Leung et al., 2018; Song et al., 2019; Zou et al., 2017). V850 in particular is a strong predictor of $PM_{2.5}$ wintertime pollution events in the North China Plain, because northerly winds (negative V850) ventilate the region with clean dry air (Cai et al., 2017; Pendergrass et al., 2019).

All data in this work are averaged over 10 days (10-day time resolution). Trend analyses use only those sites with at least 70% data coverage for each of the 6 years from 2013 to 2018. We did sensitivity tests with data coverage thresholds changing from 70% to 90% and obtained similar pollutants trends. To make the most use of available data, 70% is chosen. For the MLR model, we further average all data on a 2°×2.5° grid to increase statistical robustness following Tai et al. (2012) and Shen et al. (2017).

The 2013 Clean Air Action (Council, 2013a) identified three megacity clusters as target regions for reducing air pollution: Beijing-Tianjin-Hebei (BTH; 35-41°N, 113.75-118.75°E), Yangtze River Delta (YRD; 29-33°N, 118.75-123°E), and Pearl River Delta (PRD; 21-25°N, 111.25-116.25°E). The more recent plan released in July 2018 (Chinese State Council, 2018b) removed PRD from the list of target regions and added Fenwei Plain (FWP; 33-35°N, 106.25-111.25°E & 35-37°N, 108.75-113.75°E). Previous studies (X. Zhang et al., 2012) also identified Sichuan Basin (SCB; 27-33°N, 103.75-108.75°E) as one of the major haze regions in China. We present analyses for these five target regions by averaging the data from all sites with more than 70% data coverage for each of the 6 years from 2013 to 2018. The only continuous record for 2013-2018 in the FWP region is for Xi'an (13 sites). Additional FWP sites outside Xi'an started operating in early 2015 and are consistent with the Xi'an data, as will be shown below.

2.2.   Multiple linear regression model

We construct a stepwise multiple linear regression (MLR) model to quantify the effect of meteorology on $PM_{2.5}$ variability. The model fits the deseasonalized and detrended 10-day $PM_{2.5}$ mean time series on the 2°×2.5° grid to the five deseasonalized and detrended 10-day mean meteorological variables (WDS, PRECIP, RH, TEM, V850). The deseasonalized and detrended time series are obtained by removing the 50-day moving averages from the 10-day mean time series (Tai et al., 2010). This

focuses on synoptic scales of variability and avoids aliasing from common seasonal variations and long-term trends between variables (Shen et al., 2017).

Separate fits of PM$_{2.5}$ to the meteorological variables are done for each 2°×2.5° grid square and season (DJF, MAM, JJA, SON). The fit has the form:

$$Y_{d,i}(t) = \sum_{k=1}^{5} \beta_{i,k} X_{d,i,k}(t) + b_i \tag{1}$$

where $Y_{d,i}(t)$ is the deseasonalized and detrended PM$_{2.5}$ time series for grid square and season i, and $X_{d,i,k}(t)$ is the corresponding time series for the deseasonalized and detrended meteorological variable $k \in [1,5]$. We fit the regression coefficients $\beta_{i,k}$ and the intercept b_i. The regression is done stepwise, adding and deleting terms based on their independent statistical significance to obtain the best model fit (Drapper and Smith, 1998). The fits and the selected meteorological variables differ by location and season but with regional consistency (Table S1). For meteorological variables not in the final MLR model, the regression coefficients $\beta_{i,k}$ in equation (1) are zero.

2.3.   Application to 2013-2018 PM$_{2.5}$ trends

We use the MLR model to remove the effect of meteorological variability from the 2013-2018 PM$_{2.5}$ trends, including not only the 10-day synoptic-scale variability but also any interannual variability and 6-year trends. This makes the standard assumption that the same factors that drive synoptic-scale variability also drive interannual variability (Jacob and Winner, 2009; Tai et al., 2012). We thus apply equation (1) to the meteorological anomalies $X_{a,i,k}$, obtained by removing the 6-year means of the 50-day moving averages from the 10-day mean time series. The anomalies calculated in this manner are deseasonalized but not detrended. This yields the meteorology-driven PM$_{2.5}$ anomalies $Y_{m,i}$:

$$Y_{m,i}(t) = \sum_{k=1}^{5} \beta_{i,k} X_{a,i,k}(t) + b_i \tag{2}$$

Consider now the PM$_{2.5}$ anomaly $Y_{a,i}$ for grid square and season i obtained by deseasonalizing but not detrending the PM$_{2.5}$ data (by removing the 6-year means of the 50-day moving averages), in the same way as for the meteorological variables. The residual anomaly $Y_{r,i}$ after removing meteorological influence from the MLR model is given by

$$Y_{r,i}(t) = Y_{a,i}(t) - Y_{m,i}(t) \tag{3}$$

The residual is the component of the anomaly that cannot be explained by the MLR meteorological model and we will refer to it as the meteorology-corrected data. It includes noise due to limitations of the MLR model and other factors, but also a long-term trend over the 6-year period that we can attribute to changes in anthropogenic emissions. The same approach was recently applied by Li et al. (2019) to separate anthropogenic and meteorological drivers of ozone trends in China.

3. Results and Discussion

3.1. PM$_{2.5}$ trends in China, 2013-2018

Figure 1 shows annual mean observed PM$_{2.5}$ concentrations from the CNEMC over China for 2013 and 2018, and the linear regression trends on the 2°×2.5° grid based on the PM$_{2.5}$ anomalies $Y_{a,i}(t)$ including effects of both changing emissions and meteorology. In 2013, PM$_{2.5}$ across most of China was well above the Chinese national air quality standard (annual mean of 35 μg m^{-3}). BTH and FWP (Xi'an) had the highest PM$_{2.5}$ among the five target regions, with annual average concentrations of 108 ± 34 μg m^{-3} (standard deviation describes variability of the annual average across sites in the region) and 108 ± 11 μg m^{-3} respectively, followed by SCB (71 ± 17 μg m^{-3}), YRD (67 ± 12 μg m^{-3}), and PRD (47 ± 7 μg m^{-3}). PM$_{2.5}$ decreased dramatically from 2013 to 2018, by 34-49% for the five target regions. Mean 2018 concentrations were 55 ± 13 μg m^{-3} in BTH, 62 ± 4 μg m^{-3} in FWP (Xi'an), 40 ± 6 μg m^{-3} in SCB, 40 ± 7 μg m^{-3} in YRD, and 31 ± 5 μg m^{-3} in PRD.

Figure 2 shows the 2013-2018 relative trends of annual mean PM$_{2.5}$ for the five target regions, along with the corresponding trends of SO$_2$, NO$_2$, and CO concentrations measured at the same sites. Also shown in the bottom panels are the MEIC inventory trends in emissions of primary PM$_{2.5}$, SO$_2$, NO$_x$, NH$_3$, and CO for 2013-2017. The PM$_{2.5}$ observations show steady decreases for BTH, YRD, and SCB. PRD flattens out in 2015-2017 before decreasing again in 2018. FWP (Xi'an) decreases sharply by 47% from 2013 to 2015 but rebounds in 2015-2017 before decreasing again in 2018. Trends at other FWP sites that became operational in early 2015 are similar to Xi'an. We argue in Section 3.3 that the 2015-2017 flattening at PRD and the anomalously 2013-2015 sharp decrease and 2015-2017 rebound at FWP are driven by meteorology.

We see from Figure 2 that only SO$_2$ has a decrease steeper than PM$_{2.5}$, indicating that SO$_2$ emission controls have been a major driver of the PM$_{2.5}$ trend (Lang et al., 2017; Shao et al., 2018). The overall SO$_2$ decrease for the five regions is 57-76% from 2013 to 2018. The SO$_2$ decrease is quantitatively consistent with the decrease of SO$_2$ emissions estimated by MEIC (Zheng et al., 2018). This drastic cut of China SO$_2$ emissions is due to installation of scrubbers at coal-fired power plants (Siwen et al., 2015; Karplus et al., 2018; Silver et al., 2018), elimination of small coal boilers, improvement of coal quality (Zheng et al., 2018), and switch from residential coal to cleaner fuels (Zhao et al., 2018). We also see a significant decrease in CO of 18-43% for the five regions from 2013 to 2018, again consistent with the MEIC emission inventory and suggesting a reduction in organic PM$_{2.5}$ emissions. Primary PM$_{2.5}$ emissions in the MEIC inventory decreased at a rate comparable to or steeper than CO. Trends in China PM$_{2.5}$, SO$_2$, and NO$_2$ presented here are consistent with previous studies (Silver et al., 2018; Ma et al., 2019) that cover a shorter time period than 2013-2018.

Figure 3 shows the time series of monthly mean $PM_{2.5}$ for the five target regions, illustrating the seasonal and interannual variability. All regions show winter maxima that can be mostly attributed to meteorology including shallower mixing depth, lower precipitation, and increased stagnation in winter (X. Wang et al., 2018). Residential heating emissions in winter also contribute to the seasonality in China north of about 33°N (covering BTH and FWP in this study; J. Liu et al., 2016b; Xiao et al., 2015). There is a large interannual variability, particularly in winter, that must be largely driven by meteorology. Studies for BTH have shown that high $PM_{2.5}$ in winter months is associated with weak southerly winds, low mixing depths, and high relative humidity (R. Zhang et al., 2014; Chang et al., 2016; Li et al., 2018; Shao et al., 2018). The relatively clean 2017-2018 winter was due in part to a higher frequency of northerly flow and associated ventilation (Administration, 2018; Yi et al., 2019). In addition, particularly aggressive actions by the government to restrict coal use that winter may have played a role in reducing $PM_{2.5}$ levels (X. Zhang et al., 2019).

3.2. Meteorological influence on $PM_{2.5}$

Figure 4 shows the correlations of 10-day $PM_{2.5}$ concentrations with the individual meteorological variables used in the MLR model. Correlation coefficients r as low as 0.3 are statistically significant, and more so when consistent across a region. Wind speed is negatively correlated with $PM_{2.5}$, as would be expected from ventilation, except in areas of the north where wind promotes dust formation (Lyu et al., 2017; X. Wang et al., 2004). Precipitation is also generally negatively correlated with $PM_{2.5}$, as one would expect from scavenging (Chen et al., 2018). The positive correlation between precipitation and $PM_{2.5}$ over north China in spring is likely a result of high RH associated with precipitation in adjacent days.

Correlation between RH and $PM_{2.5}$ is positive over northern China, especially in winter, and negative over southern China, especially in summer. The positive correlation between $PM_{2.5}$ and RH over northern China in winter has been reported by previous studies and attributed in part to the role of aqueous-phase aerosol chemistry in driving secondary $PM_{2.5}$ formation (Zheng et al., 2015; He et al., 2018; Song et al., 2019; Pendergrass et al., 2019; Tie et al., 2017). The negative correlation of $PM_{2.5}$ with RH over south China likely reflects the association of high RH with precipitation and onshore wind, which facilitate $PM_{2.5}$ wet removal and ventilation (Zhu et al., 2012; Leung et al., 2018).

Temperature has a positive correlation with $PM_{2.5}$ year round over most of China (Y. Wang et al., 2014; Leung et al., 2018), even though there is no strong direct dependence of $PM_{2.5}$ on temperature (Jacob and Winner, 2009). The correlation likely reflects the covariation of temperature with other meteorological variables including wind speed, precipitation, and RH (Tai et al., 2012; Zhu et al., 2012). A possible explanation for the negative correlation with temperature in summer over North China Plain could be the volatilization of ammonium nitrate at high temperature (Kleeman, 2008). V850 shows strong

positive correlations with winter $PM_{2.5}$ over most of China, and strong negative correlations with summer $PM_{2.5}$ over south

China, especially for the Pearl River Delta.

Figure 5 (left panel) describes the ability of the MLR model to account for $PM_{2.5}$ variability in relation to wind speed, precipitation, RH, temperature, and V850 as potential predictor variables. Results are presented as the coefficients of determination R^2 (fraction of variance explained) between observed and model $PM_{2.5}$ in the detrended deseasonalized time series. The R^2 values have been adjusted to account for different numbers of significant explanatory terms (predictor variables). R^2 values for the five target regions are: 0.59 (BTH), 0.46 (YRD), 0.65(PRD), 0.65 (SCD), and 0.41 (FWP). The right panel of Figure 5 shows the meteorology-corrected $PM_{2.5}$ trends after removal of meteorological variability predicted by the MLR model, i.e., the trends in the residuals $Y_{r,i}(t)$ in equation (3). The meteorology-corrected decreasing trend averaged across China is -4.6 µg m^{-3} a^{-1}, 12% weaker than in the original data, meaning that 12% of the $PM_{2.5}$ decrease in the original data is attributable to meteorology. We elaborate below for the five target regions.

3.3. Meteorology-corrected $PM_{2.5}$ trends for the five target regions

Figure 6 shows the 10-day mean $PM_{2.5}$ anomalies in the deseasonalized (but not detrended) data for the five target regions ($Y_a(t)$ in Section 2.3). Also shown is the meteorological component $Y_m(t)$ derived from the MLR meteorological model, and the residual $Y_r(t)$ (meteorology-corrected, equation (3)) whose long-term trend can be interpreted as due to changes in anthropogenic emissions. The $PM_{2.5}$ anomalies show large features on ten-day basis that can be mostly captured by the MLR model. The residual meteorology-corrected time series is much smoother, as depicted by the narrower 95% confidence intervals in the anthropogenic residual trends than in the original observed trends. The meteorology-corrected trends differ by 3% (YRD) to 27% (SCB) from the observed trends. The YRD trend reflects a significant contribution from the December 2013 outlier, which reflects unfavorable meteorological conditions (Figure S2) that are not adequately captured by the MLR model. If we exclude this outlier month from the time series, the observed YRD trend becomes -5.7 ± 0.9 µg m^{-3} a^{-1} and the meteorology-corrected trend becomes -5.9 ± 0.7 µg m^{-3} a^{-1}.

Most remarkably, it appears that the 2015-2017 flattening in the PRD and 2015-2017 increase in the FWP (see Figure 2) can be mostly attributed to meteorological variability as resolved by the MLR model, rather than to emissions. The trend in the residual is more consistent with a steady 2013-2018 anthropogenic decrease in both regions. The MLR model shows that meteorology accelerated the $PM_{2.5}$ decline in PRD and FWP from 2013 to 2015, and contributed partly to the 2015-2017 $PM_{2.5}$ rebound over FWP. In particular, the high $PM_{2.5}$ anomalies in PRD in 2013 and early 2014 are driven by anomalously low V850, and the low $PM_{2.5}$ in winter 2015-2016 is associated with anomalously high southerly flow and precipitation

(Figure S4). The low PM$_{2.5}$ in FWP in the winter 2014-2015 is associated with anomalously high wind speed, low RH, and low temperature, while the high anomalies in the winter 2016-2017 are associated with anomalously low wind speed, high RH, and high temperature (Figure S5).

4. Conclusions

Observations of fine particulate matter (PM$_{2.5}$) pollution in China from the extensive CNEMC network established in 2013 show large 2013-2018 decreases driven by emission controls with complicating influences from meteorology. Here we used a stepwise multiple linear regression (MLR) meteorological model to investigate and separate contributions from anthropogenic emissions and meteorology to these 6-year trends.

The CNEMC observations show 34-49% decreases in PM$_{2.5}$ in the five megacity clusters targeted by the Chinese government's Clean Air Action to reduce anthropogenic emissions. Concurrent observations of SO$_2$, CO, and NO$_2$ are qualitatively consistent with these PM$_{2.5}$ decreases being driven by drastic cuts in emissions from coal combustion. At the same time, there is large interannual variability driven by meteorology particularly in winter when PM$_{2.5}$ is highest.

We used the stepwise MLR meteorological model to relate PM$_{2.5}$ anomalies across China to wind speed, precipitation, relative humidity (RH), temperature, and meridional velocity at 850 hPa (V850) as potential predictors. The model accounts for ~50% of the variance in the deseasonalized detrended PM$_{2.5}$ data, including 41-65% for the five megacity clusters. Application to the PM$_{2.5}$ time series shows that meteorological variability contributed significantly to the 6-year trends across China and in the megacity clusters. Removing meteorological variability as given by the MLR model also reduces the uncertainty in the trend that can be attributed to emission controls. We refer to the data series after removal of meteorological variability as the meteorology-corrected data. Thus the 2013-2018 PM$_{2.5}$ decrease for Beijing-Tianjin-Hebei is -9.3 ± 1.8 µg m^{-3} a^{-1} in the original data and is 14% weaker in the meteorology-corrected data (-8.0 ± 1.1 µg m^{-3} a^{-1}). For the Sichuan Basin where the meteorological correction is particularly large, the PM$_{2.5}$ decrease is -6.7 ± 1.3 µg m^{-3} a^{-1} in the original data and is reduced by 27% to -4.9 ± 0.9 µg m^{-3} a^{-1} in the meteorology-corrected data. The average 2013-2018 PM$_{2.5}$ decrease over our study domain is -5.2 µg m^{-3} a^{-1} in the original data (Figure 1 (right panel)) and is reduced by 12% to -4.6 µg m^{-3} a^{-1} in the meteorology-corrected data (Figure 5 (right panel)).

Observations for the 2015-2017 period indicate a flattening of the PM$_{2.5}$ trend in the Pearl River Delta and an increase in the Fenwei Plain. We find from the MLR model that these 3-year trends can be explained by meteorological variability (including particularly steep 2013-2015 decreases) rather than by relaxation of emission controls.

Data availability. All of the measurements, reanalysis data are openly available for download from the websites given in the main text. The anthropogenic emission inventory is available from www.meicmodel.org, and for more information, please contact Qiang Zhang (qiangzhang@tsinghua.edu.cn).

Competing interests. The authors declare that they have no conflict of interest.

Author contributions. SXZ, DJJ, and HL designed the study. SXZ developed the model, performed the simulations and analyses. XW, LS, KL, YZZ, and TLZ helped with scientific interpretation and discussion. KG helped with pollutants data processing. SXZ and DJJ wrote the manuscript and all authors provided input on the paper for revision before submission.

Acknowledgments. This work is a contribution from the Harvard-NUIST Joint Laboratory for Air Quality and Climate (JLAQC). Hong Liao is supported by the National Natural Science Foundation of China (91744311). This work was also supported by the China Scholarship Council, National Key R & D Program Pilot Projects (2016YFC0203304) and Natural Science Foundation of China (41830965 & 91744209). We thank the MEIC (Multi-resolution Emission Inventory for China) team in Tsinghua University for providing the MEIC emission inventory. We acknowledge Loretta J. Mickley (Harvard University) and Jonathan Moch (Harvard University) for helpful discussions.

5. References

Barrero, M. A., Orza, J. A. G., Cabello, M., and Canton, L.: Categorisation of air quality monitoring stations by evaluation of PM_{10} variability, Science of The Total Environment, 524-525, 225-236, https://doi.org/10.1016/j.scitotenv.2015.03.138, 2015.

Cai, W., Li, K., Liao, H., Wang, H., and Wu, L.: Weather conditions conducive to Beijing severe haze more frequent under climate change, Nature Climate Change, 7, 257-263, 2017.

Chang, L., Xu, J., Tie, X., and Wu, J.: Impact of the 2015 El Nino event on winter air quality in China, Scientific reports, 6, 34275, 2016.

Che, H., Zhang, X., Li, Y., Zhou, Z., and Qu, J. J.: Horizontal visibility trends in China 1981-2005, Geophysical Research Letters, 34, 10.1029/2007GL031450, 2007.

Chen, Z., Xie, X., Cai, J., Chen, D., Gao, B., He, B., Cheng, N., and Xu, B.: Understanding meteorological influences on $PM_{2.5}$ concentrations across China: a temporal and spatial perspective, Atmospheric Chemistry and Physics, 18, 5343-5358, 2018.

Chen, Z., Chen, D., Kwan, M., Chen, B., Cheng, N., Gao, B., Zhuang, Y., Li, R., and Xu, B.: The control of anthropogenic emissions contributed to 80 % of the decrease in $PM_{2.5}$ concentrations in Beijing from 2013 to 2017, Atmos. Chem. Phys. Discuss., 2019, 1-25, 10.5194/acp-2018-1112, 2019.

Cheng, J., Su, J., Cui, T., Li, X., Dong, X., Sun, F., Yang, Y., Tong, D., Zheng, Y., Li, Y., Li, J., Zhang, Q., and He, K.: Dominant role of emission reduction in $PM_{2.5}$ air quality improvement in Beijing during 2013-2017: a model-based decomposition analysis, Atmos. Chem. Phys., 19, 6125-6146, 10.5194/acp-19-6125-2019, 2019.

Chinese State Council. Action Plan on Air Pollution Prevention and Control, 2013a (in Chinese). http://www.gov.cn/zwgk/2013-09/12/content_2486773.htm (last access: 26 December 2018).

Chinese State Council. Release of $PM_{2.5}$ monitoring information in China, 2013b (in Chinese). http://www.gov.cn/jrzg/2013-01/01/content_2303447.htm (last access: 26 December 2018).

Chinese State Council. Full realization of the "Action Plan on Prevention and Control of Air Pollution", 2018a (in Chinese). http://www.gov.cn/xinwen/2018-02/01/content_5262720.htm (last access: 26 December 2018).

Chinese State Council. Three-year Action Plan on Defending the Blue Sky, 2018b (in Chinese). http://www.gov.cn/zhengce/content/2018-07/03/content_5303158.htm (last access: 26 December 2018)

Cohen, A. J., Brauer, M., Burnett, R., Anderson, H. R., Frostad, J., Estep, K., Balakrishnan, K., Brunekreef, B., Dandona, L., and Dandona, R.: Estimates and 25-year trends of the global burden of disease attributable to ambient air pollution: an analysis of data from the Global Burden of Diseases Study 2015, The Lancet, 389, 1907-1918, 2017.

de Foy, B., Lu, Z., and Streets, D. G.: Satellite NO_2 retrievals suggest China has exceeded its NO_x reduction goals from the twelfth Five-Year Plan, Scientific Reports, 6, 35912, 2016.

Drapper, N. R., and Smith, H.: Applied regression analysis, John Wiley & Sons, 1998.

Dunlea, E. J., Herndon, S. C., Nelson, D. D., Volkamer, R. M., San Martini, F., Sheehy, P. M., Zahniser, M. S., Shorter, J. H., Wormhoudt, J. C., Lamb, B. K., Allwine, E. J., Gaffney, J. S., Marley, N. A., Grutter, M., Marquez, C., Blanco, S., Cardenas, B., Retama, A., Ramos Villegas, C. R., Kolb, C. E., Molina, L. T., and Molina, M. J.: Evaluation of nitrogen dioxide chemiluminescence monitors in a polluted urban environment, Atmos. Chem. Phys., 7, 2691-2704, 10.5194/acp-7-2691-2007, 2007.

Fu, G. Q., Xu, W. Y., Yang, R. F., Li, J. B., and Zhao, C. S.: The distribution and trends of fog and haze in the North China Plain over the past 30 years, Atmos. Chem. Phys., 14, 11949-11958, 10.5194/acp-14-11949-2014, 2014.

Han, L., Zhou, W., and Li, W.: Fine particulate ($PM_{2.5}$) dynamics during rapid urbanization in Beijing, 1973-2013, Scientific Reports, 6, 23604, 10.1038/srep23604, 2016.

He, P., Alexander, B., Geng, L., Chi, X., Fan, S., Zhan, H., Kang, H., Zheng, G., Cheng, Y., and Su, H.: Isotopic constraints on heterogeneous sulfate production in Beijing haze, Atmospheric Chemistry and Physics, 18, 5515-5528, 2018.

Jacob, D. J., and Winner, D. A.: Effect of climate change on air quality, Atmospheric Environment, 43, 51-63, https://doi.org/10.1016/j.atmosenv.2008.09.051, 2009.

Jia, B., Wang, Y., Yao, Y., and Xie, Y.: A new indicator on the impact of large-scale circulation on wintertime particulate matter pollution over China, Atmospheric Chemistry and Physics, 15, 11919-11929, 2015.

Kang, Y., Liu, M., Song, Y., Huang, X., Yao, H., Cai, X., Zhang, H., Kang, L., Liu, X., and Yan, X.: High-resolution ammonia emissions inventories in China from 1980 to 2012, Atmospheric Chemistry and Physics, 16, 2043-2058, 2016.

Karplus, V. J., Zhang, S., and Almond, D.: Quantifying coal power plant responses to tighter SO_2 emissions standards in China, Proceedings of the National Academy of Sciences, 201800605, 2018.

Kleeman, M. J.: A preliminary assessment of the sensitivity of air quality in California to global change, Climatic Change, 87, 273-292, 2008.

Lang, J., Zhang, Y., Zhou, Y., Cheng, S., Chen, D., Guo, X., Chen, S., Li, X., Xing, X., and Wang, H.: Trends of $PM_{2.5}$ and chemical composition in Beijing, 2000-2015, Aerosol Air Qual. Res, 17, 412-425, 2017.

Leung, D. M., Tai, A. P. K., Mickley, L. J., Moch, J. M., Donkelaar, A. V., Shen, L., and Martin, R. V.: Synoptic meteorological modes of variability for fine particulate matter ($PM_{2.5}$) air quality in major metropolitan regions of China, Atmospheric Chemistry & Physics, 1-29, 2018.

Li, K., Liao, H., Cai, W., and Yang, Y.: Attribution of Anthropogenic Influence on Atmospheric Patterns Conducive to Recent Most Severe Haze Over Eastern China, Geophysical Research Letters, 45, 2072-2081, 10.1002/2017GL076570, 2018.

325 Li, K., Jacob, D. J., Liao, H., Shen, L., Zhang, Q., and Bates, K. H.: Anthropogenic drivers of 2013-2017 trends in summer surface ozone in China, Proceedings of the National Academy of Sciences, 116, 422-427, 2019.

Liang, X., Li, S., Zhang, S., Huang, H., and Chen, S. X.: $PM_{2.5}$ data reliability, consistency, and air quality assessment in five Chinese cities, Journal of Geophysical Research: Atmospheres, 121, 10,220-210,236, 10.1002/2016JD024877, 2016.

Lin, C. Q., Liu, G., Lau, A. K. H., Li, Y., Li, C. C., Fung, J. C. H., and Lao, X. Q.: High-resolution satellite remote sensing of

330 provincial PM2.5 trends in China from 2001 to 2015, Atmospheric Environment, 180, 110-116, https://doi.org/10.1016/j.atmosenv.2018.02.045, 2018.

Liu, F., Zhang, Q., Zheng, B., Tong, D., Yan, L., Zheng, Y., and He, K.: Recent reduction in NO_x emissions over China: synthesis of satellite observations and emission inventories, Environmental Research Letters, 11, 114002, 2016a.

Liu, J., Mauzerall, D. L., Chen, Q., Zhang, Q., Song, Y., Peng, W., Klimont, Z., Qiu, X., Zhang, S., Hu, M., Lin, W., Smith,

335 K. R., and Zhu, T.: Air pollutant emissions from Chinese households: A major and underappreciated ambient pollution source, Proceedings of the National Academy of Sciences, 113, 7756, 2016b.

Lu, X., Hong, J., Zhang, L., Cooper, O. R., Schultz, M. G., Xu, X., Wang, T., Gao, M., Zhao, Y., and Zhang, Y.: Severe Surface Ozone Pollution in China: A Global Perspective, Environmental Science & Technology Letters, 10.1021/acs.estlett.8b00366, 2018.

340 Lu, Z., Streets, D. G., Zhang, Q., Wang, S., Carmichael, G. R., Cheng, Y. F., Wei, C., Chin, M., Diehl, T., and Tan, Q.: Sulfur dioxide emissions in China and sulfur trends in East Asia since 2000, Atmos. Chem. Phys., 10, 6311-6331, 10.5194/acp-10-6311-2010, 2010.

Lyu, Y., Qu, Z., Liu, L., Guo, L., Yang, Y., Hu, X., Xiong, Y., Zhang, G., Zhao, M., Liang, B., Dai, J., Zuo, X., Jia, Q., Zheng, H., Han, X., Zhao, S., and Liu, Q.: Characterization of dustfall in rural and urban sites during three dust storms in

345 northern China, 2010, Aeolian Research, 28, 29-37, https://doi.org/10.1016/j.aeolia.2017.06.004, 2017.

Ma, Z., Hu, X., Sayer, A. M., Levy, R., Zhang, Q., Xue, Y., Tong, S., Bi, J., Huang, L., and Liu, Y.: Satellite-Based Spatiotemporal Trends in $PM_{2.5}$ Concentrations: China, 2004-2013, Environmental health perspectives, 124, 184-192, 10.1289/ehp.1409481, 2016.

Ma, Z., Liu, R., Liu, Y., and Bi, J.: Effects of air pollution control policies on $PM_{2.5}$ pollution improvement in China from

350 2005 to 2017: a satellite-based perspective, Atmos. Chem. Phys., 19, 6861-6877, 10.5194/acp-19-6861-2019, 2019.

Moch, J. M., Dovrou, E., Mickley, L. J., Keutsch, F. N., Cheng, Y., Jacob, D. J., Jiang, J., Li, M., Munger, J. W., and Qiao, X.: Contribution of hydroxymethane sulfonate to ambient particulate matter: A potential explanation for high particulate sulfur during severe winter haze in Beijing, Geophysical Research Letters, 2018.

Pendergrass, D. C., Shen, L., Jacob, D. J., and Mickley, L. J.: Predicting the impact of climate change on severe wintertime

355 particulate pollution events in Beijing using extreme value theory, Geophysical Research Letters, 2019.

Rohde, R. A., and Muller, R. A.: Air pollution in China: mapping of concentrations and sources, PLoS one, 10, e0135749, 2015.

Shao, P., Tian, H., Sun, Y., Liu, H., Wu, B., Liu, S., Liu, X., Wu, Y., Liang, W., Wang, Y., Gao, J., Xue, Y., Bai, X., Liu, W., Lin, S., and Hu, G.: Characterizing remarkable changes of severe haze events and chemical compositions in multi-size

360 airborne particles (PM_1, $PM_{2.5}$ and PM_{10}) from January 2013 to 2016-2017 winter in Beijing, China, Atmospheric Environment, 189, 133-144, https://doi.org/10.1016/j.atmosenv.2018.06.038, 2018.

Shen, L., Mickley, L. J., and Murray, L. T.: Influence of 2000-2050 climate change on particulate matter in the United States: results from a new statistical model, Atmospheric Chemistry and Physics, 17, 4355-4367, 2017.

Shen, L., Jacob, D. J., Mickley, L. J., Wang, Y., and Zhang, Q.: Insignificant effect of climate change on winter haze

365 pollution in Beijing, Atmos. Chem. Phys., 18, 17489-17496, 10.5194/acp-18-17489-2018, 2018.

Siwen, W., Qiang, Z., Randall, V. M., Sajeev, P., Fei, L., Meng, L., Xujia, J., and Kebin, H.: Satellite measurements oversee China's sulfur dioxide emission reductions from coal-fired power plants, Environmental Research Letters, 10, 114015, 2015.

Silver, B.; Reddington, C. L.; Arnold, S. R.; Spracklen, D. V., Substantial changes in air pollution across China during 2015-2017. Environmental Research Letters 2018, 13 (11), 114012.

Song, S., Gao, M., Xu, W., Sun, Y., Worsnop, D. R., Jayne, J. T., Zhang, Y., Zhu, L., Li, M., Zhou, Z., Cheng, C., Lv, Y., Wang, Y., Peng, W., Xu, X., Lin, N., Wang, Y., Wang, S., Munger, J. W., Jacob, D. J., and McElroy, M. B.: Possible heterogeneous chemistry of hydroxymethanesulfonate (HMS) in northern China winter haze, Atmos. Chem. Phys., 19, 1357-1371, 10.5194/acp-19-1357-2019, 2019.

Tai, A. P. K., Mickley, L. J., and Jacob, D. J.: Correlations between fine particulate matter ($PM_{2.5}$) and meteorological variables in the United States: Implications for the sensitivity of $PM_{2.5}$ to climate change, Atmospheric Environment, 44, 3976-3984, https://doi.org/10.1016/j.atmosenv.2010.06.060, 2010.

Tai, A. P. K., Mickley, L. J., Jacob, D. J., Leibensperger, E. M., Zhang, L., Fisher, J. A., and Pye, H. O. T.: Meteorological modes of variability for fine particulate matter ($PM_{2.5}$) air quality in the United States: implications for $PM_{2.5}$ sensitivity to climate change, Atmospheric Chemistry and Physics, 12, 3131-3145, 2012.

Tao, J., Zhang, L., Zhang, R., and Cao, J.: A review of current knowledge concerning $PM_{2.5}$ chemical composition, aerosol optical properties, and their relationships across China, Atmospheric Chemistry & Physics, 2017, 1-70, 2017.

Tie, X., Huang, R.-J., Cao, J., Zhang, Q., Cheng, Y., Su, H., Chang, D., Poschl, U., Hoffmann, T., Dusek, U., Li, G., Worsnop, D. R., and O'Dowd, C. D.: Severe Pollution in China Amplified by Atmospheric Moisture, Scientific Reports, 7, 15760, 10.1038/s41598-017-15909-1, 2017.

van der A, R. J., Mijling, B., Ding, J., Koukouli, M. E., Liu, F., Li, Q., Mao, H., and Theys, N.: Cleaning up the air: effectiveness of air quality policy for SO_2 and NO_x emissions in China, Atmos. Chem. Phys., 17, 1775-1789, 10.5194/acp-17-1775-2017, 2017.

Wang, H. J., and Chen, H. P.: Understanding the recent trend of haze pollution in eastern China: roles of climate change, Atmos. Chem. Phys., 16, 4205-4211, 10.5194/acp-16-4205-2016, 2016.

Wang, J., Zhao, B., Wang, S., Yang, F., Xing, J., Morawska, L., Ding, A., Kulmala, M., Kerminen, V.-M., Kujansuu, J., Wang, Z., Ding, D., Zhang, X., Wang, H., Tian, M., Petaja, T., Jiang, J., and Hao, J.: Particulate matter pollution over China and the effects of control policies, Science of The Total Environment, 584-585, 426-447, https://doi.org/10.1016/j.scitotenv.2017.01.027, 2017.

Wang, X., Dong, Z., Zhang, J., and Liu, L.: Modern dust storms in China: an overview, Journal of Arid Environments, 58, 559-574, 2004.

Wang, X., Dickinson, R. E., Su, L., Zhou, C., and Wang, K.: $PM_{2.5}$ pollution in China and how it has been exacerbated by terrain and meteorological conditions, Bulletin of the American Meteorological Society, 99, 105-119, 2018.

Wang, Y., Yao, L., Wang, L., Liu, Z., Ji, D., Tang, G., Zhang, J., Sun, Y., Hu, B., and Xin, J.: Mechanism for the formation of the January 2013 heavy haze pollution episode over central and eastern China, Science China Earth Sciences, 57, 14-25, 2014.

Xia, Y., Zhao, Y., and Nielsen, C. P.: Benefits of China's efforts in gaseous pollutant control indicated by the bottom-up emissions and satellite observations 2000-2014, Atmospheric Environment, 136, 43-53, 2016.

Xiao, Q., Ma, Z., Li, S., and Liu, Y.: The impact of winter heating on air pollution in China, PloS one, 10, e0117311, 2015.

Xu, P., Liao, Y. J., Lin, Y. H., Zhao, C. X., Yan, C. H., Cao, M. N., Wang, G. S., and Luan, S. J.: High-resolution inventory of ammonia emissions from agricultural fertilizer in China from 1978 to 2008, Atmospheric Chemistry and Physics, 16, 1207-1218, 2016.

Yang, Y., Liao, H., and Lou, S.: Increase in winter haze over eastern China in recent decades: Roles of variations in meteorological parameters and anthropogenic emissions, Journal of Geophysical Research: Atmospheres, 121, 13,050-013,065, 10.1002/2016JD025136, 2016.

Yang, Y., Wang, H., Smith, S. J., Zhang, R., Lou, S., Qian, Y., Ma, P.-L., and Rasch, P. J.: Recent intensification of winter haze in China linked to foreign emissions and meteorology, Scientific reports, 8, 2107, 2018.

Yi, K., Liu, J., Wang, X., Ma, J., Hu, J., Wan, Y., Xu, J., Yang, H., Liu, H., Xiang, S., and Tao, S.: A combined Arctic-tropical climate pattern controlling the inter-annual climate variability of wintertime PM2.5 over the North China Plain, Environmental Pollution, 245, 607-615, https://doi.org/10.1016/j.envpol.2018.10.136, 2019.

Zhang, R., Li, Q., and Zhang, R.: Meteorological conditions for the persistent severe fog and haze event over eastern China in January 2013, Science China Earth Sciences, 57, 26-35, 10.1007/s11430-013-4774-3, 2014.

Zhang, X. Y., Wang, Y. Q., Niu, T., Zhang, X. C., Gong, S. L., Zhang, Y. M., and Sun, J. Y.: Atmospheric aerosol compositions in China: spatial/temporal variability, chemical signature, regional haze distribution and comparisons with global aerosols, Atmospheric Chemistry and Physics, 12, 779-799, 2012.

Zhang, X. Y., Xu, X. D., Ding, Y. H., Liu, Y. J., Zhang, H. D., Wang, Y. Q., Zhong, J. T.: The impact of meteorological changes from 2013 to 2017 on PM2.5 mass reduction in key regions in China, Science China Earth Sciences, 49, doi: 10.1360/N072018-00303, 2019.

Zhang, Y.-L., and Cao, F.: Fine particulate matter (PM$_{2.5}$) in China at a city level, Scientific Reports, 5, 14884, 10.1038/srep14884, https://www.nature.com/articles/srep14884#supplementary-information, 2015.

Zhao, B., Jonathan, H. J., Yu, G., David, D., John, W., Kuo-Nan, L., Hui, S., Jia, X., Michael, G., and Lei, H.: Decadal-scale trends in regional aerosol particle properties and their linkage to emission changes, Environmental Research Letters, 12, 054021, 2017.

Zhao, B., Zheng, H., Wang, S., Smith, K. R., Lu, X., Aunan, K., Gu, Y., Wang, Y., Ding, D., and Xing, J.: Change in household fuels dominates the decrease in PM2. 5 exposure and premature mortality in China in 2005-2015, Proceedings of the National Academy of Sciences, 115, 12401-12406, 2018.

Zheng, B., Zhang, Q., Zhang, Y., He, K. B., Wang, K., Zheng, G. J., Duan, F. K., Ma, Y. L., and Kimoto, T.: Heterogeneous chemistry: a mechanism missing in current models to explain secondary inorganic aerosol formation during the January 2013 haze episode in North China, Atmospheric Chemistry and Physics (Online), 15, 2015.

Zheng, B., Tong, D., Li, M., Liu, F., Hong, C., Geng, G., Li, H., Li, X., Peng, L., and Qi, J.: Trends in China's anthropogenic emissions since 2010 as the consequence of clean air actions, Atmospheric Chemistry and Physics, 18, 14095-14111, 2018.

Zhu, J., Liao, H., and Li, J.: Increases in aerosol concentrations over eastern China due to the decadal-scale weakening of the East Asian summer monsoon, Geophysical Research Letters, 39, 10.1029/2012GL051428, 2012.

Zou, Y., Wang, Y., Zhang, Y., and Koo, J.-H.: Arctic sea ice, Eurasia snow, and extreme winter haze in China, Science Advances, 3, e1602751, 10.1126/sciadv.1602751, 2017.

Annual mean PM$_{2.5}$ concentrations and trends, 2013-2018
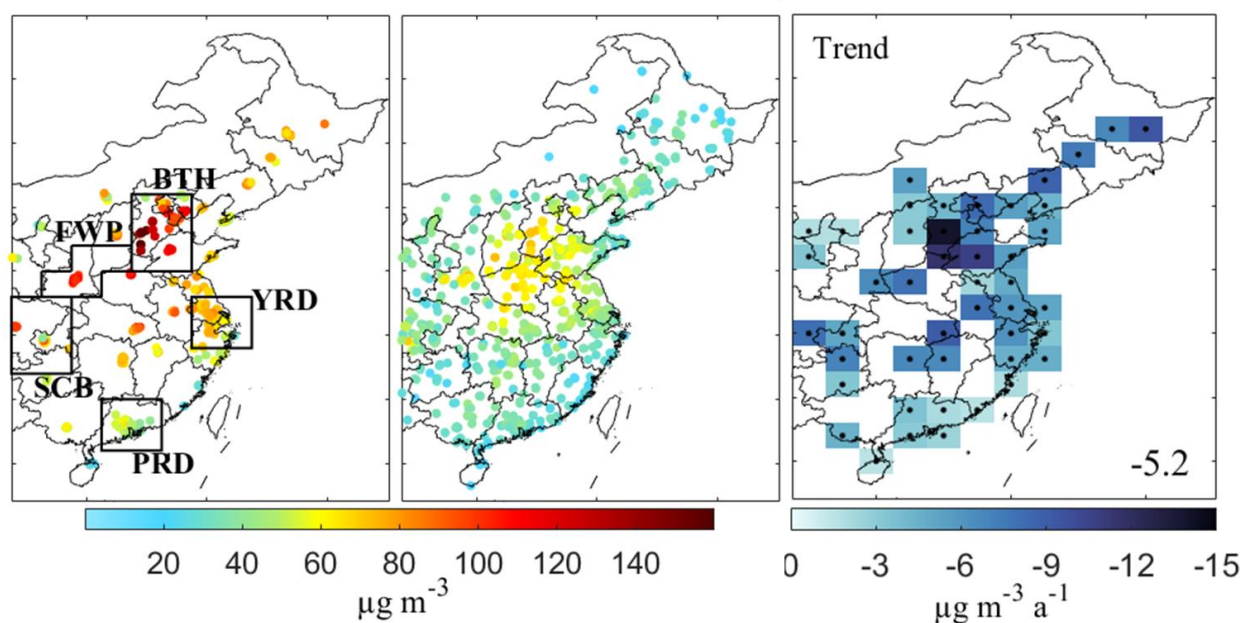
Figure 1 Annual mean PM$_{2.5}$ concentrations in China from the CNEMC network. Left and middle panels show values for 2013 and 2018 for sites with more than 70% data coverage for the corresponding year. The right panel shows the ordinary linear regression trends on a 2°x2.5° grid for sites with more than 70% data coverage for each of the six years from 2013 to 2018. The trends are based on the timeseries of 10-day mean anomalies as described in the text. Polygons in the left panel define the four target regions of the Clean Air Action (Beijing-Tianjin-Hebei (BTH; 35-41°N, 113.75-118.75°E), Yangtze River Delta (YRD; 29-33°N, 118.75-123°E), Pearl River Delta (PRD; 21-25°N, 111.25-116.25°E), and Fenwei Plain (FWP; 33-35°N, 106.25-111.25°E & 35-37°N, 108.75-113.75°E)), to which we add Sichuan Basin (SCB; 27-33°N, 103.75-108.75°E). Number inset in the right panel is the trend in mean PM$_{2.5}$ over the study region (21-41°N, 103.75-123°E). Dots in the right panel indicate grid squares with significant trends ($p < 0.05$).
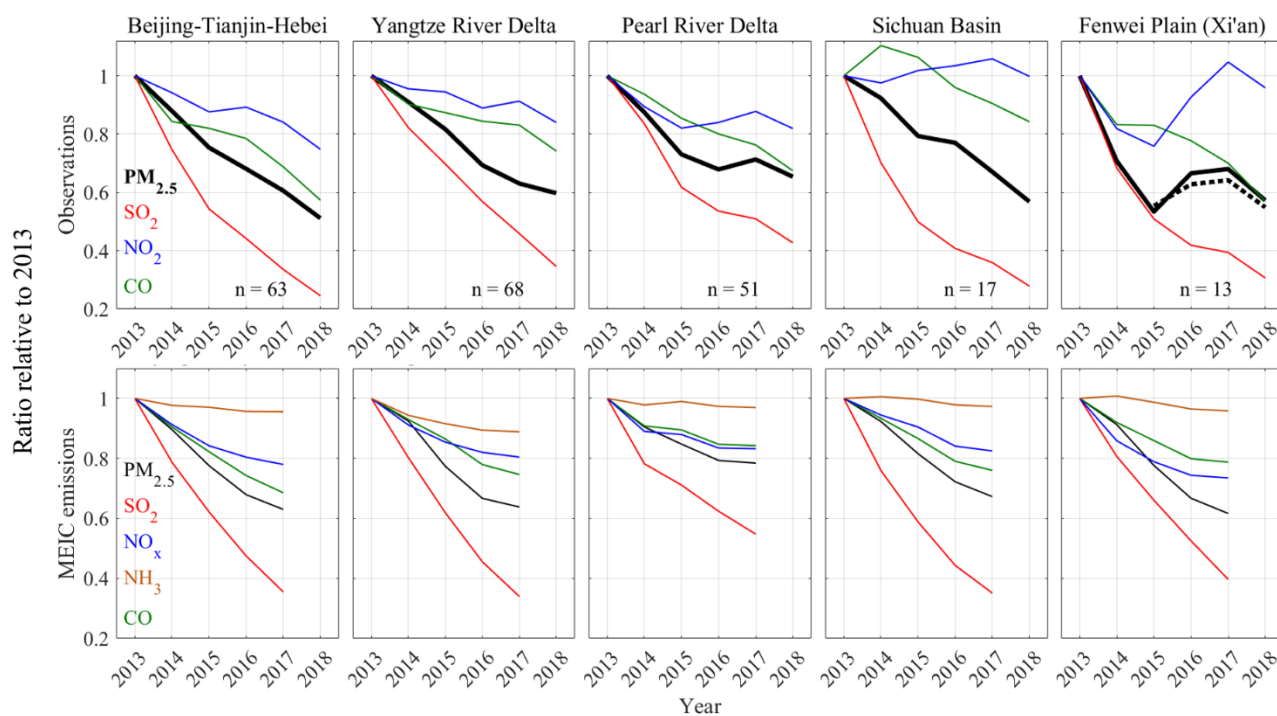
Figure 2. Relative trends of 2013-2018 observed concentrations and 2013-2017 MEIC emission estimates for the five target regions of Figure 1. The observed PM$_{2.5}$ trends are shown as thick lines. Values are annual means referenced to 2013. The observed concentrations are averaged over all sites in each region with at least 70% data coverage for each year. The number of sites for each region is indicated. Fenwei Plain trends are for Xi'an as other sites did not start operating until early 2015. Post-2015 relative PM$_{2.5}$ trends at these other sites are shown as the dashed line.

455

460
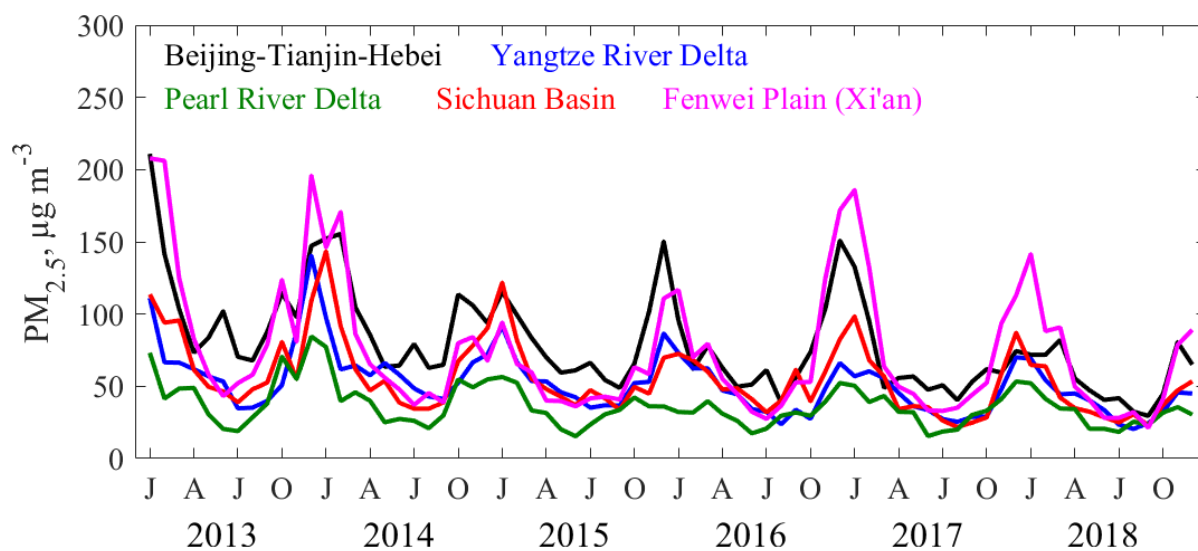
Figure 3 2013-2018 time series of monthly mean PM$_{2.5}$ concentrations over the five target regions. Values are averages from all sites in the region with over 70% data coverage for each of the six years.
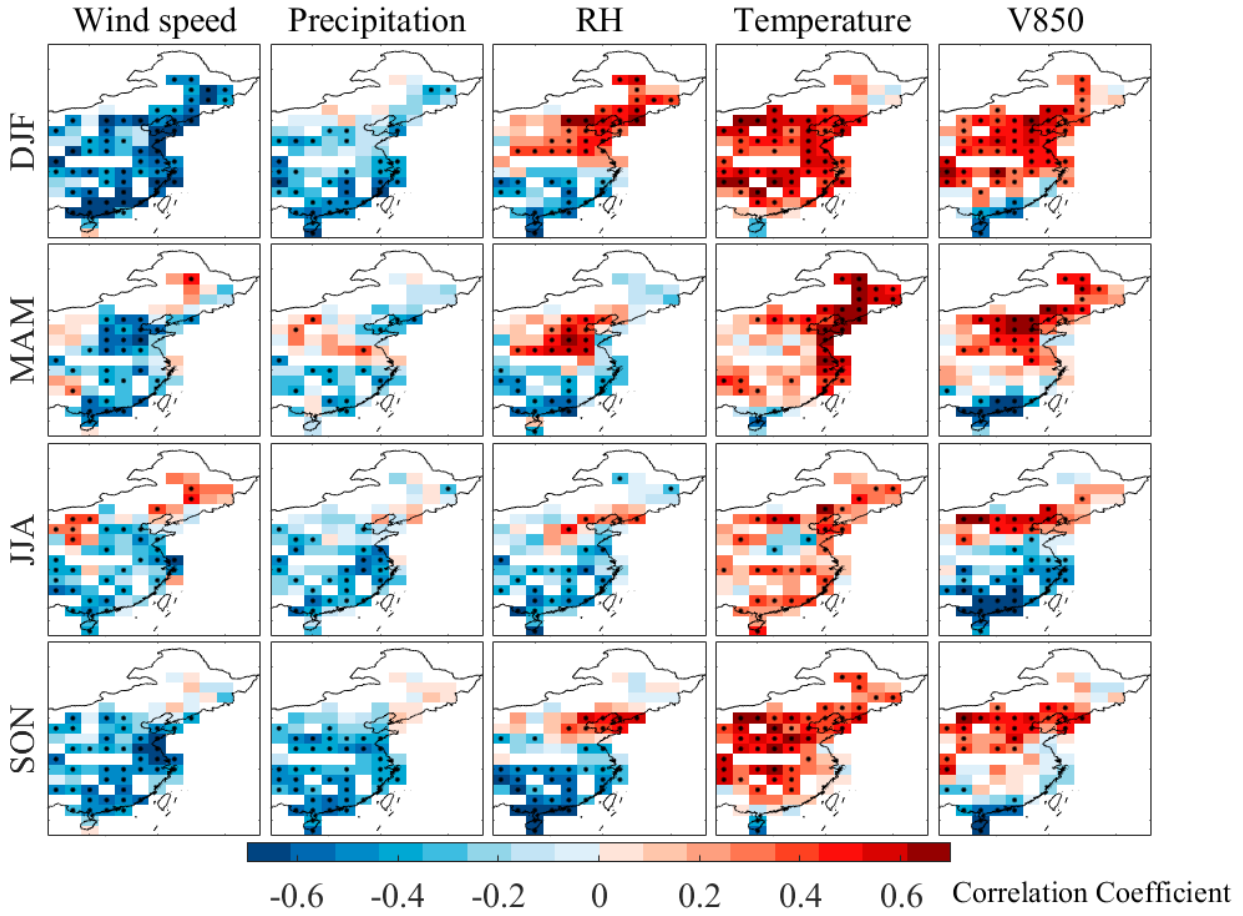
Figure 4 Correlation coefficients (*r*) of PM₂.₅ concentration with the individual meteorological variables used in the MLR model: surface wind speed (m s⁻¹), precipitation (mm d⁻¹), relative humidity (RH; %), surface air temperature (°C), and 850hPa meridional wind velocity (m s⁻¹) for different seasons in China. The correlations are based on 10-day average observations on a 2°×2.5° grid. Dots indicate statistically significant correlations (*p* < 0.05).

470
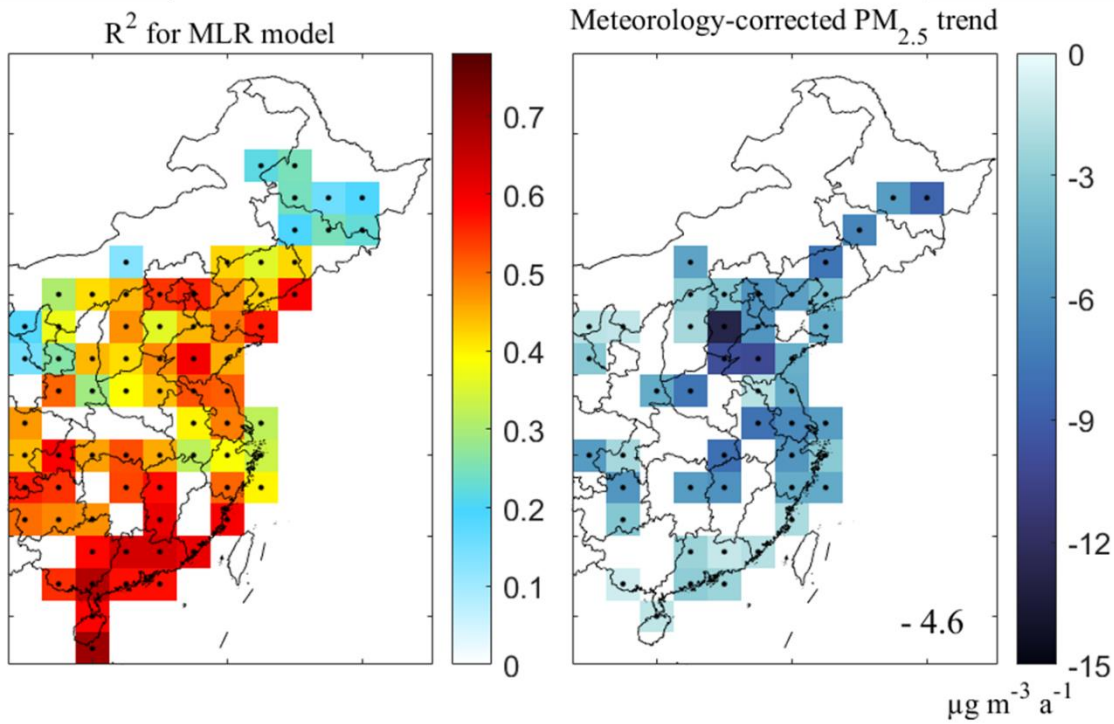
Figure 5 Resolving meteorological influences on PM$_{2.5}$ 2013-2018 trends in China. The left panel shows the fraction of detrended and deseasonalized variance in 10-day PM$_{2.5}$ means explained by the stepwise multi linear regression (MLR) meteorological model. The right panel shows the meteorology-corrected trends, to be compared to the trends in the original data shown in Figure 1. Number inset in the right panel is the trend in mean PM$_{2.5}$ over the study region (same definition as in Figure 1). Dots indicate

475   **significant correlations ($p < 0.05$) in the left panel and significant trends ($p < 0.05$) in the right panel.**
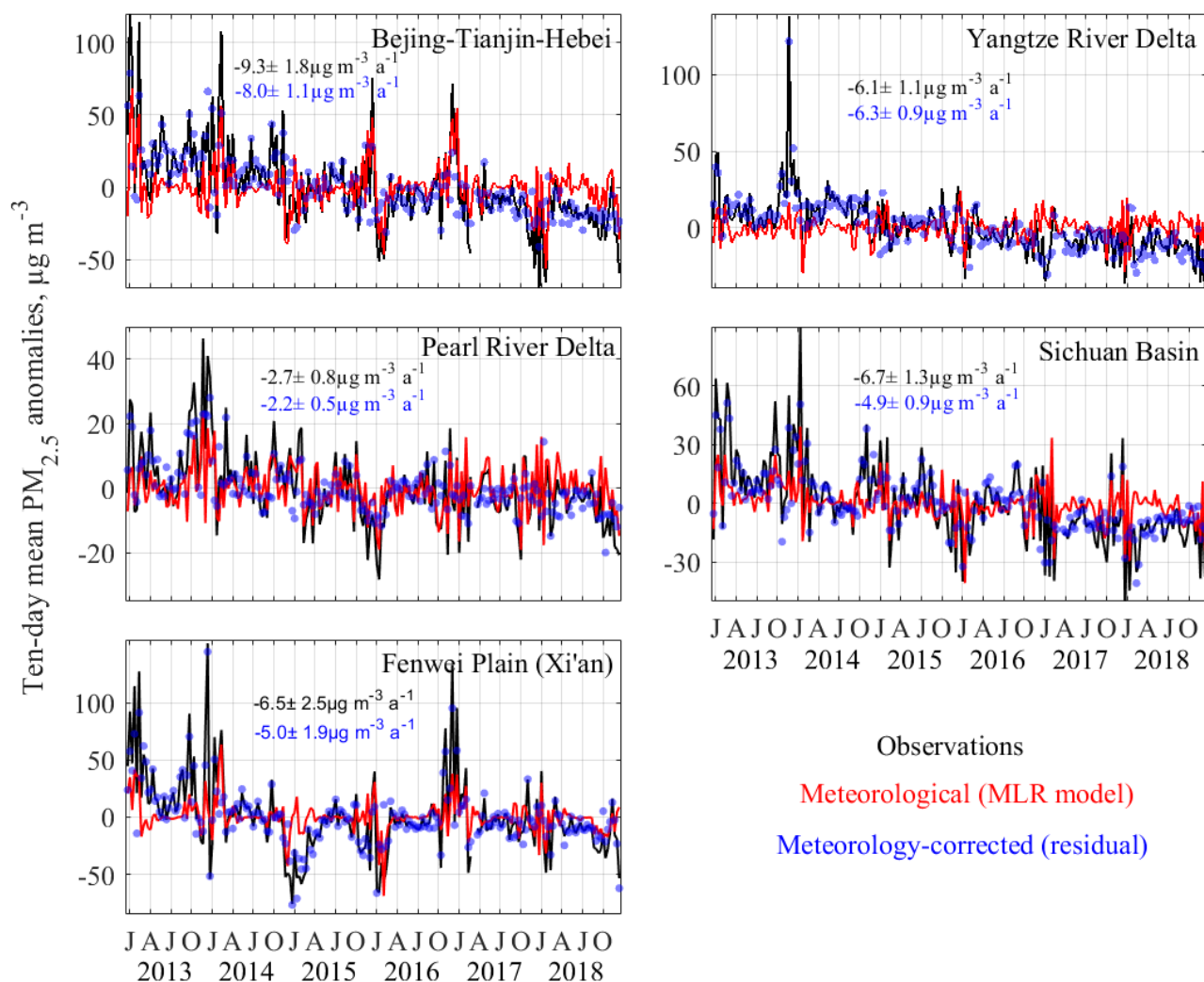
Figure 6. Time series of 2013-2018 PM₂.₅ 10-day mean anomalies for the five target regions of Figure 1. The anomalies are relative to the 2013-2018 means. The data are averaged over all measurement sites in each region with at least 70% of data coverage for each year (same as for Figure 2). The meteorological contribution to the anomalies as diagnosed from the MLR model is shown in red. The long-term trend in the meteorology-corrected residual in blue (equation (3)) is interpreted as driven by changes in anthropogenic emissions. Values inset each panel are the ordinary linear regression trends with 95% confidence intervals obtained by the bootstrap method.